Observability of 2π rotations: A proposed experiment

A. G. Klein and G. I. Opat
School of Physics, University of Melbourne, Parkville, Victoria 3052, Australia
(Received 26 September 1974)

Rotations by 2π radians of spin-$\frac{1}{2}$ systems are predicted to give rise to factors of -1 in the wave function. We propose an experiment involving Fresnel diffraction of thermal neutrons to test this proposition.

I. INTRODUCTION

A rotation of 2π radians about an arbitrary axis performed on an *isolated* physical system is believed to be an identity operation on that system. By this we mean that no experimental test carried out on the rotated system will show that it was in fact rotated. This belief is incorporated in both the classical and quantum mechanics of isolated systems, and reflects the assumed isotropy of free space.

However, the commonly held proposition, that *all rotations through 2π radians performed on a physical system are undetectable,* is open to challenge. It has been pointed out independently by Aharonov and Susskind[1] and by Bernstein[2] that quantum-mechanical theory predicts that there can be observable consequences of a 2π-radian rotation applied to a half-integral-spin system.[3] When a system of half-integral spin is rotated through 2π radians, quantum mechanics predicts[4] that the phase of its wave function changes by -1. Under normal circumstances this -1 is completely lost, as all observable quantities are quadratic in the wave function. However, if the wave function is split into two parts, one part coherently rotated through 2π radians relative to the other, it develops a relative phase of -1. On subsequent reconstruction of the two parts of the wave function, the interference pattern will show considerable modification due to the relative phase factor of -1. This proposition has never been tested by direct experiment.

After outlining the theory in further detail, we put forward a concrete proposal for a simple experiment with thermal neutrons to test for the predicted effect.

II. THEORY

Let $\vec{\alpha}$ be the vector angle of rotation, i.e., $\alpha \equiv |\vec{\alpha}|$ is the magnitude of the rotation and $\hat{\alpha}$ is the unit axis vector about which the rotation occurs in a right-handed sense. The rotation operation of quantum mechanics for an arbitrary system is given by

$$R(\vec{\alpha}) = \exp(-i\vec{\alpha}\cdot\vec{J}), \tag{1}$$

where $\vec{J}$ is the angular momentum operator.[4] For a spin-$\frac{1}{2}$ system $R(\vec{\alpha})$ is represented by the 2×2 matrix $\underline{r}(\vec{\alpha})$, given by

$$\underline{r}(\vec{\alpha}) = \exp(-i\vec{\alpha}\cdot\vec{\underline{\sigma}}/2)$$
$$= \underline{1}\cos\tfrac{1}{2}\alpha - i\hat{\alpha}\cdot\vec{\underline{\sigma}}\sin\tfrac{1}{2}\alpha, \tag{2}$$

where $\underline{\sigma}_i$ denotes a Pauli spin matrix. As usual, a spinor wave function ψ transforms according to

$$\psi(x) \to \psi'(x) = \underline{r}(\vec{\alpha})\psi(M^{-1}(\vec{\alpha})\vec{x}), \tag{3}$$

where $M(\vec{\alpha})$ is the 3×3 matrix which rotates vectors.

If $\alpha = 2\pi$ with $\hat{\alpha}$ arbitrary, then

$$\underline{r}(2\pi\hat{\alpha}) = -\underline{1}, \tag{4}$$

so that a rotation of 2π about an arbitrary axis leads to

$$\psi(\vec{x}) \to \psi'(\vec{x}) = -\psi(\vec{x}). \tag{5}$$

Therefore, the effect of a complete rotation on the *entire* spinor wave function of a spin-$\frac{1}{2}$ system is to alter its phase by -1. As all observable quantities, such as position or polarization, are quadratic in the wave function, this factor of -1 does not appear in any such quantities. (This argument holds for all half-integral-spin systems.)

The situation is completely different if only a *part* of a spinor wave function is rotated. Let S denote a region of ordinary three-dimensional space. Let $\Delta(\vec{x})$, $\bar{\Delta}(\vec{x})$ denote the functions with the following properties:

$$\Delta(\vec{x}) = 1, \quad \bar{\Delta}(\vec{x}) = 0 \quad (\text{if } \vec{x} \in S), \tag{6a}$$

$$\Delta(\vec{x}) = 0, \quad \bar{\Delta}(\vec{x}) = 1 \quad (\text{if } \vec{x} \notin S). \tag{6b}$$

It follows that

$$\Delta(\vec{x}) + \bar{\Delta}(\vec{x}) = 1, \tag{6c}$$

$$\Delta(\vec{x})\bar{\Delta}(\vec{x}) = 0. \tag{6d}$$

Consider a 2-component spinor wave function $\psi(\vec{x})$ and the unitary operation $\underline{U}(\vec{\alpha}, \vec{x})$ defined by

$$\underline{U}(\vec{\alpha},\vec{x}) \equiv \bar{\Delta}(\vec{x})\underline{1} + \Delta(\vec{x})\underline{r}(\vec{\alpha}) . \tag{7}$$

This operation rotates the internal structure (i.e., spin) of a particle through angle $\vec{\alpha}$ when it lies in S, and leaves it alone otherwise. Let

$$\begin{aligned}\psi'(\vec{x}) &= U(\vec{\alpha},\vec{x})\psi(\vec{x}) \\ &= \bar{\Delta}(\vec{x})\psi(\vec{x}) + \Delta(\vec{x})\underline{r}(\alpha)\psi(\vec{x}) .\end{aligned} \tag{8}$$

If $\vec{\alpha} = 2\pi\hat{\alpha}$, then

$$U(2\pi\hat{\alpha},\vec{x}) \equiv U(\vec{x}) = \bar{\Delta}(\vec{x}) - \Delta(\vec{x}) , \tag{9a}$$

$$\psi(\vec{x}) \to \psi'(\vec{x}) = \bar{\Delta}(\vec{x})\psi(\vec{x}) - \Delta(\vec{x})\psi(\vec{x}) . \tag{9b}$$

We note that the position probability distribution and polarization vector are left unchanged by this transformation:

$$|\psi(\vec{x})|^2 \to |\psi'(\vec{x})|^2 = |\psi(\vec{x})|^2 , \tag{10a}$$

$$\psi^\dagger \underline{\vec{\sigma}} \psi \to \psi'^\dagger \underline{\vec{\sigma}} \psi' = \psi^\dagger \underline{\vec{\sigma}} \psi . \tag{10b}$$

For experimental reasons it is more desirable to rotate the two parts of the wave function through angles π in opposite senses, i.e., through a relative angle of 2π. This may be described by the unitary operator $V(\vec{x})$,

$$\begin{aligned}V(\vec{x}) &\equiv \underline{r}(-\pi\hat{\alpha})\bar{\Delta}(\vec{x}) + \underline{r}(\pi\hat{\alpha})\Delta(\vec{x}) \\ &= \underline{r}(-\pi\hat{\alpha})[\bar{\Delta}(\vec{x}) + \underline{r}(2\pi\hat{\alpha})\Delta(\vec{x})] \\ &= \underline{r}(-\pi\hat{\alpha})[\bar{\Delta}(\vec{x}) - \Delta(\vec{x})] \\ &= \underline{r}(-\pi\hat{\alpha})U(\vec{x}) .\end{aligned} \tag{11}$$

We see that the -1 in question appears again, as the operator $V(\vec{x})$ is equivalent to the operation $U(\vec{x})$, followed by a rotation $-\pi\hat{\alpha}$. Any wave in the region S(or $\bar{S}$) will diffract out of that region in the course of time. Thus, the waves formerly in S and $\bar{S}$ will interfere with each other, making the relative phase change observable.

If $K(\vec{x}t|\vec{x}'t')$ denotes the Green function for time evolution and

$$\phi(\vec{x}t) \equiv \int d^3x' K(\vec{x}t|\vec{x}'t')\Delta(\vec{x}')\psi(\vec{x}'t') , \tag{12a}$$

$$\bar{\phi}(\vec{x}t) \equiv \int d^3x' K(\vec{x}t|\vec{x}'t')\bar{\Delta}(\vec{x}')\psi(\vec{x}'t') , \tag{12b}$$

then the proposed experiment can be symbolized by the sequence

$$\begin{aligned}\psi(\vec{x}t') \to V(\vec{x})\psi(\vec{x}t') &= \underline{r}(-\pi\hat{\alpha})[\bar{\Delta}(\vec{x})\psi(\vec{x}t') - \Delta(\vec{x})\psi(\vec{x}t')] \\ &\to \underline{r}(-\pi\hat{\alpha})[\bar{\phi}(\vec{x}t) - \phi(\vec{x}t)] ,\end{aligned} \tag{13}$$

giving the probability density

$$|\psi(\vec{x}t')|^2 \to |\bar{\phi}(\vec{x}t) - \phi(\vec{x}t)|^2 . \tag{14}$$

For a relative rotation of 0 or 4π, the relative phase would be $+1$ giving

$$|\psi(\vec{x}t')|^2 \to |\psi(\vec{x}t)|^2 = |\bar{\phi}(\vec{x}t) + \phi(\vec{x}t)|^2 , \tag{15}$$

leading to a detectable difference.

Pure spin rotation can be achieved by precessing the magnetic moment $\vec{\mu}$ of an uncharged spin-$\frac{1}{2}$ particle in a magnetic field $\vec{B}$. If a particle spends time t in the magnetic field, the time evolution of its spin is given by

$$T = \exp(i\vec{\mu}\cdot\vec{B}t/\hbar) . \tag{16}$$

Writing $\vec{\mu}$ in terms of the gyromagnetic ratio γ,

$$\vec{\mu} = \gamma\hbar\vec{\sigma}/2 , \tag{17}$$

we may equate T with the rotation matrix $\underline{r}(\vec{\alpha})$ given in Eq. (2). Thus,

$$\vec{\alpha} = -\gamma\vec{B}t , \tag{18}$$

and for particles of speed v passing through a magnetic-field region of thickness d, we have

$$\vec{\alpha} = -\gamma\vec{B}d/v . \tag{19}$$

III. PROPOSED EXPERIMENT

A. Outline

The availability of high fluxes of thermal neutrons makes them an obvious choice for an experimental test of the above proposition. Since the aim is to observe relative phase shifts, a situation of coherent superposition has to be set up. That is to say, some kind of interferometer is required, in one arm of which the neutron spins may be rotated relative to the other arm by an angle of 2π. The neutron interferometers of the type developed by Maier-Leibnitz *et al.*[5] or Rauch *et al.*,[6] although difficult to set up and align, would in principle be suitable. Another approach, however, may give more direct results and requires apparatus which is easier to set up. We propose a Fresnel diffraction experiment with thermal neutrons in which the diffracting object is the boundary between two regions carrying opposite magnetic fields. By Ampère's circuital law, such a boundary necessarily carries an electric current. In principle, therefore, a ribbon carrying a free current would do. The large current (~ 100 A) and small dimensions (~ 10 μm) required make this somewhat impractical. However, the boundary between two domains in a ferromagnetic crystal (in the form of a foil) has precisely the right properties. For example, the alloy Fe-3%Si, commonly used in transformer laminations, is obtainable with large grains containing straight domain walls several mm in length. (Their observation using polarized neutron beams has recently been demonstrated by Schlenker and Shull.[7]) Assuming internal fields of ~ $2T$, the thickness of specimen required to precess the spins of thermal neutrons by π is of the order of 35 μm. Foils of this thickness are readily obtainable and, being several orders of magni-

tude thinner than the scattering length, are completely transparent to thermal neutrons. The Bloch wall separating two domains of opposite magnetization is only a few tens of nm in width. Such a foil is therefore an almost ideal phase object for Fresnel diffraction. The proposed setup is shown schematically in Fig. 1.

An incident beam of unpolarized, monochromatic neutrons from a high-flux reactor is defined by a narrow slit made of cadmium with gadolinium jaws. The beam is diffracted by a ferromagnetic foil in which two oppositely magnetized domains meet at a boundary, accurately aligned to be parallel to the direction of the slit.

B. Diffraction pattern

The resultant diffraction pattern may be thought of as the coherent superposition of two Fresnel straight-edge (or half-plane) patterns. The relative phase shift between the two half planes, due to the rotated spins, gives rise to an over-all pattern characterized by a central minimum. For the case of a relative phase shift of π (predicted to occur for a relative rotation of spins by 2π) there will be a null at the center of the pattern. Zero relative phase shift (expected to correspond to a relative rotation of 4π) will, of course, result in a uniform distribution of neutrons in the plane of observation. The expected patterns for these two cases are shown in Fig. 2. By tilting the foil about the x axis the effective thickness through which the neutrons travel may be adjusted. In particular, if the thickness of the specimen is chosen for relative precession angles of 2π, a tilt through 60° will produce relative precession angles of 4π allowing a complete verification of the effect sought for.

In general, the expected pattern is easily calculated in an ideal, unpolarized but coherent situation, using standard Fresnel diffraction theory. It is given by

$$I(u) = \tfrac{1}{2}(1+\cos\tfrac{1}{2}\alpha) + (1-\cos\tfrac{1}{2}\alpha)J(u),$$

where α is the relative angle of precession and

$$J(u) \equiv \mathcal{C}^2(u) + \mathcal{S}^2(u).$$

$\mathcal{C}(u)$ and $\mathcal{S}(u)$ are the standard Fresnel integrals defined by

$$\mathcal{C}(u) + i\mathcal{S}(u) \equiv \int_0^u \exp(i\pi z^2/2)\,dz .$$

The scale factors relating distances to the normalized variable u are given by

$$\frac{x}{u} = \left(\frac{\lambda ab}{2(a+b)}\right)^{1/2} \quad \text{(in the object plane)}$$

and

$$\frac{X}{u} = \left(\frac{a+b}{a}\right)\frac{x}{u} = \left[\frac{\lambda b}{2}\left(1+\frac{b}{a}\right)\right]^{1/2}$$

(in the plane of observation).

We remark on the fact that the scale of the pattern depends on $\sqrt{\lambda}$ rather than λ, and would thus be only $(400\text{ nm}/0.4\text{ nm})^{1/2} \sim 30$ times smaller for thermal neutrons than the equivalent pattern in a diffraction experiment with visible light.

Considerations of flux and detector resolution have led to the following choices for the over-all dimensions of the apparatus: $a = 0.2$ m; $b = 1.8$ m. These lead to the following scale factors for a neutron wavelength of 0.4 nm: $x/u = 6$ μm (this is the half-width of the central Fresnel zone in the object plane) and $X/u = 60$ μm. The two peaks, on either side of the central minimum in the pattern, occur at $u \sim \pm 1.2$ and should therefore appear ~ 140 μm apart in the plane of observation.

C. Coherence requirements

The central minimum in the pattern is quite insensitive to chromatic effects. For a complete thermal spectrum of incident neutrons the relative intensity is expected to dip to ~35% in the center of

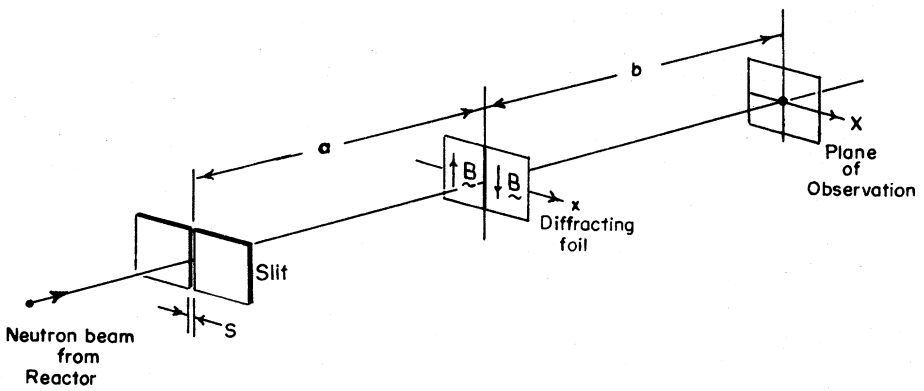

FIG. 1. Schematic layout of apparatus. Thermal and magnetic shields not shown.

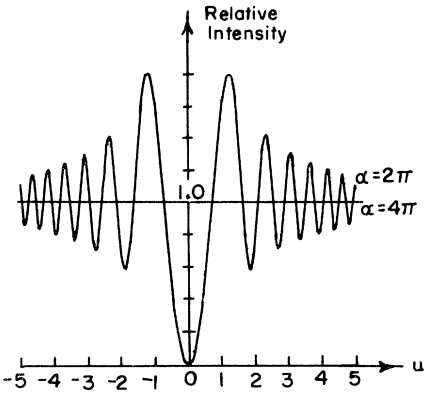

FIG. 2. Expected diffraction patterns from a coherent point source.

the pattern [for $\alpha(\langle\lambda\rangle)=2\pi$]. This is analogous to white light fringes in the equivalent optical situation. It is important, however, to preserve the difference between the patterns expected for relative precession angles α of 2π (null) and 4π (flat) and therefore a more restricted range of wavelengths has to be used. (Nevertheless, the full thermal beam may be used for alignment and testing.)

Two different conditions of monochromatization have been investigated in detail, viz., (i) a flat distribution of $\delta\lambda/\lambda=5\%$ (approximating a crystal monochromator) and (ii) the tail of the Maxwellian distribution for $\lambda>0.4$ nm, i.e.,

$$\frac{d\phi}{d\lambda}=\begin{cases}0\,, & \lambda<0.4\text{ nm}\\ (2\lambda_T^4/\lambda^5)\exp[-(\lambda_T/\lambda)^2]\,, & \lambda>0.4\text{ nm}\,,\end{cases}$$

where $\lambda_T=h/(2mk_BT)^{1/2}$ for $T=400\,^\circ$K.

This latter case corresponds to a beam obtained either by filtering the beam through a polycrystalline beryllium block or by total external reflection from a low-angle mirror. The results, combined with those of the spatial coherence calculations, will be presented below.

Spatial coherence considerations impose a critical restriction on the slit size and have been investigated with care. Broadly speaking, the requirement is that the slit width must be smaller than the width of the first Fresnel zone (strip) in the object plane (i.e., $s<2x/u=12$ μm for the dimensions chosen above). The expected patterns for various slit sizes were calculated by subdividing the slit and summing the intensities of patterns obtained from each slit division. A slit width of 5 or 6 μm was selected on this basis. The results are shown in Figs. 3 and 4 for a slit width of 6 μm and for the two different conditions of monochromaticity discussed above. In either case the distinction between precession angles $\alpha=2\pi$ and $\alpha=4\pi$ is easily discerned. The broad features of the calculated patterns were verified by an optical-analog experiment described in the Appendix.

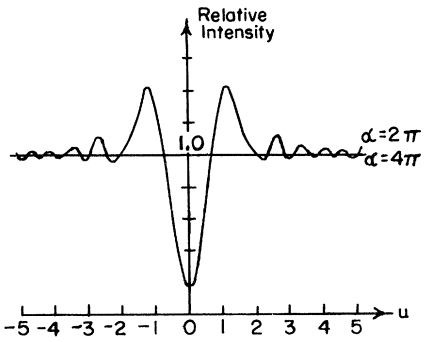

FIG. 3. Diffraction patterns for finite slit size ($u=1$) and wavelength spread of $\delta\lambda/\lambda=5\%$.

D. Detection technique

The pattern may be scanned by a second slit[5] placed in front of a conventional BF_3 counter. Alternatively, a photographic method may be used. In the first case the required spatial resolution would lead to excessively low counting rates and difficulties of alignment. Existing photographic techniques, on the other hand (using ^{7}Li-loaded ZnS scintillator and Polaroid film[8] or Gd-backed x-ray film[9]), give very poor spatial resolution—around 100 μm—or extremely low efficiency.

The track-etch technique,[10] adapted by one of the authors[11] for this specific purpose, affords a good compromise between efficiency and spatial resolution and retains the advantage of the photographic technique of not requiring any alignment. The detector consists of a plastic film on a backing of ^{10}B. The α particles from the $^{10}B(n,\alpha)$ reaction (and to some extent the ^{7}Li recoil nuclei) leave tracks of radiation damage in the plastic which may be rendered visible by chemical etching. The etched tracks (3–5 μm in diameter) are easily

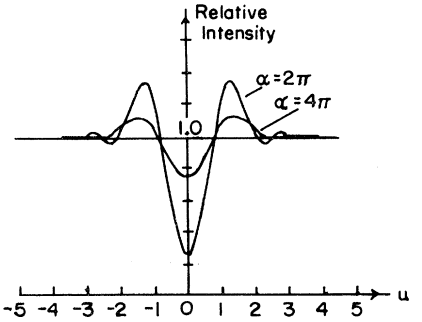

FIG. 4. Diffraction patterns for finite slit size ($u=1$) and wavelength spread corresponding to the tail ($\lambda\geq0.4$ nm) of a 400 °K Maxwellian distribution.

counted with a low-powered optical microscope. The spatial resolution is comparable with the range of α particles in the boron target or in the plastic (~ 5 μm). The expected pattern, with the central peaks separated by ~ 140 μm, should therefore be comfortably resolved by this technique. The measured efficiency (i.e., fraction of incident neutrons that leave a track) for neutrons with $\lambda = 0.1$ nm is around 5% and is expected to be somewhat greater at $\lambda = 0.4$ nm.

E. Flux calculation

The neutron current per unit area of target situated at a distance l from an entrance slit of area A is given by

$$\phi_2 = \left(\int \frac{d^2\phi_1}{d\Omega\, d\lambda}\, d\lambda \right) \frac{A_1}{l^2} ,$$

where $d^2\phi_1/d\Omega\, d\lambda$ is the flux per unit solid angle per unit wavelength interval which illuminates the entrance slit.

Typical figures for the quantity in parentheses are as follows: HIFAR,[12] thermal beam filtered by beryllium,

$$\int_{\lambda_0 = 0.4\,\mathrm{nm}}^{\infty} \frac{d^2\phi}{d\Omega\, d\lambda}\, d\lambda \sim 3 \times 10^9 \text{ neutrons cm}^{-2}\,\text{sr}^{-1};$$

HFR,[13] cold source, monochromated to $\lambda = 0.4$ nm with $\delta\lambda/\lambda \sim 5\%$,

$$\int_{\lambda_0 = 0.4\,\mathrm{nm}}^{\lambda_0 + \delta\lambda} \frac{d^2\phi}{d\Omega\, d\lambda}\, d\lambda \sim 10^{12} \text{ neutrons cm}^{-2}\,\text{sr}^{-1}.$$

For an entrance slit measuring 5 μm $\times$ 1 cm and a slit to target distance $l = (a+b) = 2.0$ m, we therefore expect on the target

$\phi_2 \sim 32$ neutrons cm^{-2}sec^{-1} (HIFAR, filtered beam)

or

$\phi_2 \sim 12\,000$ neutrons cm^{-2}sec^{-1} (HFR, monochromated, cold beam).

For the pattern to be clearly discernible, we estimate that, at most, 10^6 counts/cm^2 are required. (This was confirmed by a Monte Carlo simulation of the process which produced the pattern shown in Fig. 5.) With a counting efficiency of 5% this leads to the following estimates for the exposure time required to carry out the experiment:

$t \sim 10^6$ sec (HIFAR),

or

$t \sim 3600$ sec (HFR).

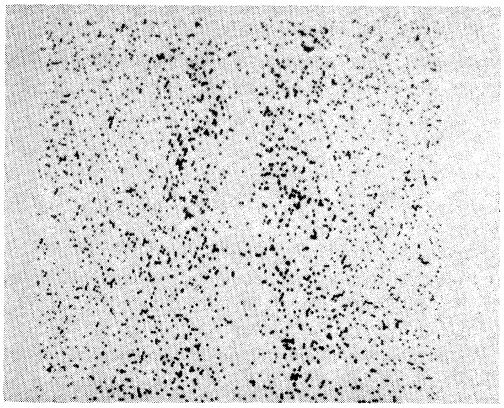

FIG. 5. Computer simulation of detected pattern with 10^6 tracks per cm^2. Area shown is 0.6 mm $\times$ 0.6 mm.

IV. CONCLUSION

The apparatus required to carry out this experiment is under construction. Preliminary runs, to test alignment, mechanical stability, thermal stability and magnetic shielding, will be carried out at HIFAR in the near future. It is hoped that facilities at the HFR will be made available to carry out the final experiments.

ACKNOWLEDGMENTS

We wish to thank Y. Ne'eman for drawing our attention to the problem, and T. M. Sabine for advice on neutron diffraction. A grant from the Australian Institute of Nuclear Science and Engineering is gratefully acknowledged.

APPENDIX: AN OPTICAL ANALOG

The diffraction aspects of the proposed experiment have been verified using visible light as follows: Plates of quartz, cut perpendicular to the optic axis out of left- and right-handed crystals, were joined side by side in optical contact along a boundary perpendicular to the incident light. The composite crystal was held between optical flats and the intervening space filled with a liquid of matching refractive index. It was then illuminated with a beam of unpolarized light defined by a variable slit.

Naturally, in the case of light, a relative phase factor of -1 occurs when the planes of polarization are rotated by π radians relative to each

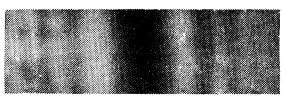

FIG. 6. Photograph of pattern obtained from the optical-analog experiment described in the Appendix.

other. Therefore, the wavelength of light was chosen so that the crystal plates produced optical rotations of $\pm\pi/2$. (For a thickness of 2.5 mm this corresponds to $\lambda \sim 470$ nm.)

The resultant diffraction pattern, seen in Fig. 6, corresponds closely to the one calculated in the text. Coherence effects were studied by varying the slit size.

[1]Y. Aharonov and L. Susskind, Phys. Rev. 158, 1237 (1967).
[2]H. J. Bernstein, Phys. Rev. Lett. 18, 1102 (1967).
[3]Epistemological criticisms of Ref. 1 by G. C. Hegefeldt and K. Kraus [Phys. Rev. 170, 1185 (1968)] were refuted by R. Mirman [Phys. Rev. D 1, 3349 (1970)].
[4]E. P. Wigner, *Group Theory and its Application to the Quantum Mechanics of Atomic Spectra* (Academic, New York, 1959, translated from the German edition of 1931), Chaps. 15 and 20.
[5]H. Maier-Leibnitz and T. Springer, Z. Phys. 167, 386 (1962). See also F. J. Landkammer, *ibid.* 189, 113 (1966); P. Korpiun, *ibid.* 195, 146 (1966).
[6]H. Rauch, W. Treimer, and U. Bonse, Phys. Lett. 47A, 369 (1974).
[7]M. Schlenker and C. G. Shull, J. Appl. Phys. 44, 4181 (1973).
[8]S. P. Wang, C. G. Shull, and W. C. Phillips, Rev. Sci. Instrum. 33, 126 (1962).
[9]H. Berger, Annu. Rev. Nucl. Sci. 21, 335 (1971).
[10]R. L. Fleischer, P. B. Price, and R. M. Walker, Nucl. Sci. Eng. 22, 153 (1965).
[11]A. G. Klein (unpublished).
[12]High Flux Australian Reactor, AAEC Research Establishment, Lucas Heights, New South Wales.
[13]High Flux Reactor, Institut Laue-Langevin, Grenoble, France.

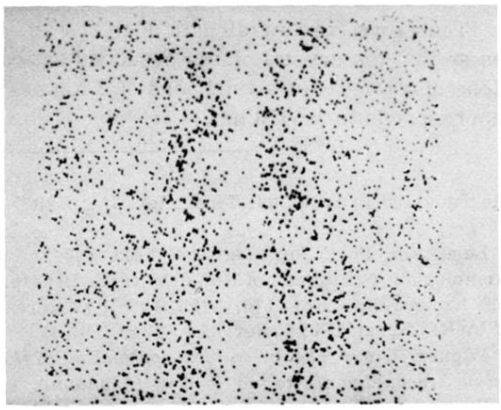

FIG. 5. Computer simulation of detected pattern with 10^6 tracks per cm^2. Area shown is 0.6 mm $\times$ 0.6 mm.

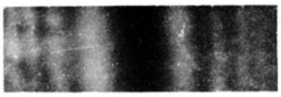

FIG. 6. Photograph of pattern obtained from the optical-analog experiment described in the Appendix.